Published in final edited form as:
Nat Mater. 2008 July ; 7(7): 539–542. doi:10.1038/nmat2209.

CHARGE ORDER FLUCTUATIONS IN ONE-DIMENSIONAL SILICIDES

Changgan Zeng[1], **P. R.C. Kent**[2], **Tae-Hwan Kim**[2], **An-Ping Li**[2], and **Hanno H. Weitering**[1,3]

[1]Department of Physics and Astronomy, The University of Tennessee, Knoxville, TN 37996, USA

[2]Center for Nanophase Materials Sciences, Oak Ridge National Laboratory, Oak Ridge, Tennessee 37831, USA

[3]Materials Science and Technology Division, Oak Ridge National Laboratory, Oak Ridge, TN 37831, USA

Abstract

Metallic nanowires are of great interest as interconnects in future nanoelectronic circuits. They also represent important systems for understanding the complexity of electronic interactions and conductivity in one-dimension. We have fabricated exceptionally long and uniform YSi_2 nanowires via self-assembly of yttrium atoms on Si(001). The thinnest wires represent one of the closest realizations of the isolated Peierls chain, exhibiting van-Hove type singularities in the one-dimensional density of states and charge order fluctuations below 150 K. The structure of the wire was determined though a detailed comparison of scanning tunneling microscopy data and first-principles calculations. Sporadic broadenings of the wires' cross section imply the existence of a novel metal-semiconductor junction whose electronic properties are governed by the finite-size- and temperature-scaling of the charge ordering correlation.

One-dimensional (1D) conductors have always captured the imagination of physicists. While a strictly 1D material remains a theoretical construct, a vast number of materials can be viewed as quasi 1D, making them interesting test cases for theoretical predictions and nanoscale applications. Classic examples include charge transfer complexes such as TTF-TCNQ and the Bechgaard salts, which have been studied extensively because of their unusual electrical properties and potential applications as organic conductors (1). These compounds can be viewed as macroscopic ensembles of weakly-coupled quantum chains. They are also textbook illustrations of the venerable Peierls theorem, which states that a 1D metallic chain should be unstable with respect to a symmetry-lowering modulation of the atomic coordinates and valence-charge density (2). The mechanism driving this instability entails the strong coupling between the vibrational modes of the lattice and electrons near the Fermi level. The ground state of a Peierls chain is insulating but the band gap decreases with increasing temperature and metallicity is ultimately restored via a second order phase transition.

This simple picture contains some interesting caveats. First of all, the Peierls theory ignores thermodynamic fluctuations. In the 1D limit, thermal fluctuations always destroy long-range order so in principle there is no phase transition (3). Paradoxically, 2D or 3D interchain coupling appears essential for observing the Peierls phase transition in real systems (3).

Secondly, the Peierls theory completely ignores electron-electron correlations. Depending on the various interaction parameters, the Peierls transition may be preempted by a competing 'many-body' ground state such as a spin density wave state or Luttinger liquid (1–3). To date, the closest experimental realization of a 1D model system is, arguably, the single-wall carbon nanotube (4–7). Yet, there is no experimental evidence of a Peierls distortion in nanotubes, possibly because the tube diameters are not small enough for observing the transition (5–7). Some experiments even suggest the existence of a competing superconducting ground state (8). It is evident that fundamental understanding of 1D cooperative phenomena would greatly benefit from the availability of new materials systems approaching the 1D limit.

Here we report on the formation and electronic properties of epitaxial YSi_2 nanowires. The observed aspect ratios and large interchain distance suggest that these nanowires are among the closest experimental approximations of an isolated Peierls chain. The wires form via self-assembly after depositing approximately 0.5 monolayer (ML) of yttrium onto an atomically clean Si(001) surface at about 600°C. Fig. 1A shows a room temperature (RT) scanning tunneling microscope (STM) image of nanowires with cross-sections of about 0.4×1.1 nm^2 and lengths approaching one micrometer. Most of the yttrium is consumed by an yttrium-induced surface reconstruction or 'wetting layer' while the remainder is incorporated into the nanowires. Rare-earth silicide nanowires on Si(001) have a similar appearance (9–13), but the YSi_2 wires appear to have higher aspect ratios and better uniformity.

The close-up STM image in Fig. 1B reveals atomic resolution on the wires (the theoretical simulation of this image shown in Fig. 1C will be discussed later). Fig. 1D shows the corresponding cross-sectional height profile. The image and cross-sectional line profile can be rationalized by considering the epitaxial relationship between the hexagonal AlB_2-type structure (Fig. 2A) of the bulk silicide and the Si(001) substrate, as observed for the rare-earth silicide wires (9–13). In this scenario, the AlB_2-type structure grows in the $(11\bar{0}0)$ plane orientation with its $[11\bar{2}0]$ direction aligned parallel to one of the $<11\bar{0}>$ axes of the Si(001) substrate (Fig. 2B). For the rare-earth elements, this produces a close lattice match along the silicide's $[11\bar{2}0]$ direction (< 2%), whereas the typical lattice mismatch along the orthogonal [0001] direction is ~ 4–9%. This anisotropic strain is likely responsible for the strongly anisotropic silicide growth, producing long nanowires that extend along the $Si<11\bar{0}>$ directions (14). The present case of yttrium is unique, however, in that the misfit along the wire direction vanishes almost completely (< 0.07% at 300 K).

The YSi_2 nanowires in Fig. 1 are too thin to be subjected to transmission electron microscopy studies. Therefore, in order to determine their most likely structure we performed periodic supercell density functional (DFT) calculations using the plane-wave projector augmented wave method within the local density approximation (LDA) (15, 16). Our slab geometries contained nine Si layers, with the bottom two layers held fixed at the theoretical bulk positions and rear surface passivated with hydrogen atoms. The wetting layer was not explicitly included due to the considerable uncertainty in its likely structure and composition. The smallest AlB_2-type structure unit compatible with the STM observations consists of two parallel Si dimer rows where the Y atoms are located

underneath the dimers and possibly in the troughs between the dimer rows (Fig. 2B). The minimal wire width equals 11.5 Å which is three times the lattice spacing along the Si < $1\bar{1}0$ > direction. The structure of this '$3a_{Si}$-wide' wire obtained from fully atomistically relaxed calculations is shown in Fig. 2B. The calculated nanowire has a height of ~0.34 nm and a width of ~1.3 nm, consistent with the STM cross-sectional line profile in Fig. 1D.

To further corroborate this structural model we simulated the filled-state STM image on the $3a_{Si}$-wide wire surface, as shown in Fig. 1C. It reproduces the experimental STM image of the wire quite well, as shown in Fig. 1B. Bright protrusions represent silicon dimers, similar to the dimer rows on the clean Si(001)2×1 surface. We also performed a series of total energy calculations to verify the presence of the central yttrium atom, which cannot be resolved in the experimental images. We tested various geometries by repositioning the central yttrium atom (Fig. 2B) elsewhere on the surface at a maximum distance from the wire. In all cases we found higher energy configurations, supporting the structural model of Fig 2. The $3a_{Si}$ structures are also energetically favored compared to wires in which the central yttrium atom has been removed and returned to an yttrium reservoir at the bulk chemical potential. Alternative structures, such as those with a long period vacancy modulation along the wire or those that would break the mirror plane symmetry, would likely be visible in STM. Finally, to check the role of the surface structure in between the wires, we saturated all dangling bonds in between the wires with hydrogen. This did not noticeably change the total energy minimized structure and computed spectra (below) of the wires.

To explore the electronic properties of the wires, we performed scanning tunneling spectroscopy (STS). The tunneling I-V spectra reveal a step wise increases of the tunneling current (Fig. 2C: inset). Similar step-like features have been observed in the tunneling spectra of single-wall carbon nanotubes, consistent with the expected van Hove singularities in the 1D density of states (DOS) (17–19). This is most clearly seen in the derivative spectra, which directly reflect the 1D-DOS. Here, we compare the numerical derivative of the I–V spectrum with the calculated surface DOS for the $3a_{Si}$-wide wire (purple line in Fig. 2C). The main features of the experimental dI/dV spectra are remarkably well reproduced by the theoretical calculation, lending strong support for the structure model in Fig. 2B. Examination of the calculated electronic structure reveals that the STS peaks derive from tunneling through near-band edge hybridized Y-Si *sp* states that are localized along the wire while decaying into the bulk substrate, as shown in Fig. 2, D and E. The surface DOS was also calculated after removing the central yttrium atoms. The spectra shifted significantly (~0.3 eV) which again confirms the presence of the central yttrium atom in Fig. 2B. The experimental I–V spectra clearly indicate that the nanowires are metallic at RT.

At 40 K, images of the $3a_{si}$-wide (11.5 Å) wires exhibit bright protrusions along the wire direction, indicative of a new charge-density corrugation (Fig. 3A). The spacing between neighboring maxima fluctuates but typically corresponds to four or five Si lattice spacings. Fig. 3, B and C, shows registry aligned dual bias images. The line profiles of the images in Fig. 3D reveal that the corrugations in the filled- and empty-states are mostly out of phase, which is a hallmark of charge ordering (20). STS data also show a small energy gap of about 0.15 eV across the Fermi level (T = 40 K). The gap opening is consistent with the picture of

1D charge ordering or Peierls distortion. Interestingly, this distortion could not be captured by DFT calculations.

The fluctuations in the locations of the charge density maxima seen in filled state images are compiled in a histogram (Fig. 3E). It is clear that the spacings are not uniform, reflecting a lack of long range charge order along the wires. It is likely that the spatial fluctuations in the silicide nanowires can be attributed to the lack of interchain coupling. The average spacing and width of the spacing distribution both increase with temperature. This may be due to increased thermal fluctuations and possibly the involvement of several competing wave vectors. Fluctuating charge order can be observed up to about 150 K.

The $3a_{si}$-wide (11.5 Å) wires dominate for Y coverages up to 0.4–0.5 ML (90%); the remaining 10% wires are $5a_{si}$-wide (19.2 Å), and occasionally $7a_{si}$-wide (26.9 Å). The heights are all the same. At 40 K, charge ordering can only be observed on the $3a_{si}$-wide nanowires in Fig. 3A, while the adjacent $5a_{si}$-wide nanowire does not reveal charge ordering. Fig. 3, F and G, show atomically resolved STM images of the $5a_{si}$-wide and a $7a_{si}$-wide wires at 40 K, respectively. Interestingly, the periodicity along the wire of the $5a_{si}$-wide and $7a_{si}$-wide has doubled, compared to the $3a_{si}$-wide wires. Such $2a_{si}$ periodicity has also been observed on $DySi_2$ nanowires (13). This $2a_{si}$ periodicity is not related to charge ordering, however, because the corrugations in filled and empty states are perfectly in phase. It thus appears that at 40 K, charge ordering only occurs in wires with the smallest $3a_{si}$ cross section.

Strictly speaking, the Peierls picture only pertains to infinitely long chains. In finite systems, charge density correlations are expected to increase in amplitude as the wire length approaches a critical length or ‘coherence length’ (21, 22). For a multi-channel 1D conductor, the coherence length is estimated to be of the order of $\frac{\nu\nu_F}{2\Delta}$, where ν_F is the Fermi velocity and 2 Δ the energy gap in the highest subband channel (21). Using the computed band structure values of $\hbar\nu_F$ of ~2eVÅ, and experimental value of 2 Δ (0.15 eV), we estimate a critical length of roughly 13Å for the $3a_{Si}$-wide nanowires. This is consistent with observations of complete charge ordering in wire segments as short as 16.9 and 4.6 nm as shown in Fig. 4, A and B, respectively.

Our observations provide clear evidence for short-range charge order in 1D chains that are electronically decoupled from neighboring chains and from the semiconducting substrate. They capture a rare glimpse in real space into the destruction of 1D charge order at higher temperature. Still, it is unclear whether the charge ordering transition is driven by electron-phonon coupling or ‘Kohn anomaly’, as in the conventional Peierls picture (1–3). We observed several Fermi level crossings in the metallic band structure but there is no direct correlation between the observed charge ordering periodicities and Fermi wave vectors. This observation, along with the short coherence length and relatively large band gap, suggests that the system is best described as a strong-coupling charge density wave system showing strong phase fluctuations below the mean field transition temperature (22). The latter is estimated to be of the order of 500 °C and the charge-ordering transition is expected to be of the order-disorder type (22). Nonetheless, in this scenario the ×4 or ×5 ordered

superstructure would normally be captured by a DFT total energy minimization (23). We tested calculated structures for instabilities, perturbing the atomic positions in supercells containing up to ten wire periods, or ~1000 atom supercells. In all cases, atoms relaxed back to their original positions and no superstructure was found. Since Peierls-type instabilities are particularly delicate (24), we cannot totally exclude the possibility that a more extensive investigation or different supercells would reveal one. However, it is very likely that the observed charge ordering is sensitive to enhanced correlations in 1D systems and, consequently, poorly described by LDA-DFT.

Occasionally, the wires exhibit discrete variations in width. Fig. 4C shows a RT STM image of a 'junction' between a $3a_{si}$-wide and $5a_{si}$-wide nanowire, along with the corresponding STM line profile. The periodicity along the wire has doubled on the $5a_{si}$-wide side, consistent with our observation on individual $5a_{si}$-wide nanowires. Fig. 4D shows a similar junction at 40 K. Charge order fluctuations only develop on the $3a_{si}$-wide side of the junction, as is clearly revealed by the corresponding line profile. STS (not shown) reveals a metallic I–V spectrum on the $5a_{si}$-wide side and an insulating one on the $3a_{si}$-wide side. This 1D Schottky barrier device can be controlled by varying the temperature around the charge ordering transition. These remarkable nanowires with built-in junctions illustrate how the finite-size- and temperature-scaling behavior of a collective phenomenon may one-day be exploited in novel nano-architectures.

Acknowledgments

We thank Z.Y. Zhang and G.M. Stocks for many stimulating discussions. The experimental research was sponsored by the National Human Genome Research Institute, National Institutes of Health Grant R01HG002647, and by the Center for Nanophase Materials Sciences at Oak Ridge National Laboratory, which is sponsored by the Division of Scientific User Facilities, U.S. Department of Energy. The computational research involved resources from the National Energy Research Scientific Computing Center, which is supported by the Office of Science of the U.S. Department of Energy under Contract No. DE-AC02-05CH11231, and from the National Center for Computational Sciences at Oak Ridge National Laboratory, which is supported by the Office of Science of the US Department of Energy under Contract DE-AC05-00OR22725.

References and Notes

1. Grüner, G. Density Waves in Solids. ed. 1. Reading, MA: Addison-Wesley; 1994.
2. Peierls, RE. Quantum Theory of Solids. Oxford: Oxford University Press; 1955.
3. Berlinsky AJ. Rep. Prog. Phys. 1979; 42:1243.
4. Charlier JC, Blasé X, Roche S. Rev. Mod. Phys. 2007; 79:677.
5. Connétable D, Rignanese G-M, Charlier J-C, Blasé X. Phys. Rev. Lett. 2005; 94:015503. [PubMed: 15698095]
6. Barnett R, Demler E, Kaxiras E. Phys. Rev. B. 2005; 71:035429.
7. Piscanec S, Lazzeri M, Robertson J, Ferrari AC, Mauri F. Phys. Rev. B. 2007; 75:035427.
8. Tang ZK, Zhang L, Wang N, Zhang XX, Wen GH, Li GD, Wang JN, Chan CT, Sheng P. Science. 2001; 292:2462. [PubMed: 11431560]
9. Preinesberger C, Vandré S, Kalka T, Dähne-Prietsch M. J. Phys. D: Appl. Phys. 1998; 31:L43.
10. Chen Y, Ohlberg DAA, Medeiros-Ribeiro G, Chang YA, Williams RS. Appl. Phys. Lett. 2000; 76:4004.
11. Chen Y, Ohlberg DAA, Williams RS. J. Appl. Phys. 2002; 91:3213.
12. Preinesberger C, Becker SK, Vandré S, Kalka T, Dähne M. J. Appl. Phys. 2002; 91:1695.
13. Liu BZ, Nogami J. J. Appl. Phys. 2003; 93:593.

14. Pradhan A, Ma N-Y, Liu F. Phys. Rev. B. 2004; 70:193405.
15. Blöchl PE. Phys. Rev. B. 1994; 50:17953.
16. Kresse G, Joubert J. Phys. Rev. B. 1999; 59:1758.
17. Wildöer JWG, Venema LC, Rinzler AG, Smalley RE, Dekker C. Nature. 1998; 391:59.
18. Kim P, Odom TW, Huang J, Lieber CM. Phys. Rev. Lett. 1999; 82:1225.
19. Venkataraman L, Lieber CM. Phys. Rev. Lett. 1999; 83:5334.
20. Carpinelli JM, Weitering HH, Plummer EW, Stumpf R. Nature. 1996; 381:398.
21. Urban DF, Stafford CA, Grabert H. Phys. Rev. B. 2007; 75:205428.
22. Aruga T. Surf. Sci. Reports. 2006; 61:283.
23. González C, Flores F, Ortega J. Phys. Rev. Lett. 2006; 96:136101. [PubMed: 16712004]
24. König G, Stollhoff G. Phys. Rev. Lett. 1990; 65:1239. [PubMed: 10042210]

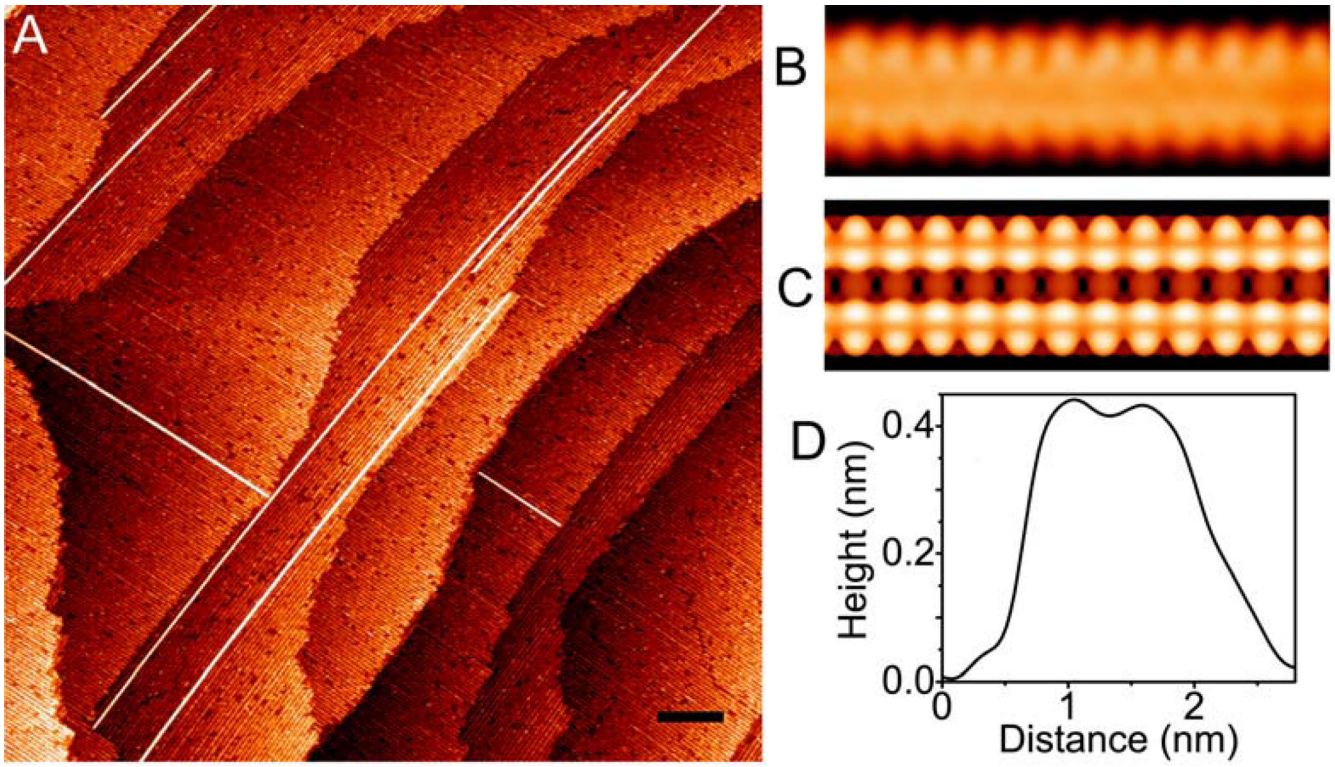

Fig. 1.

(A) Large scale STM image of self-assembled YSi_2 nanowires on Si(001), scanned at RT with a sample bias V_s of 1 V. The scale bar corresponds to 50 nm. (B) High resolution filled-state STM image scanned at RT, resolving rows of silicon dimers on a $3a_{Si}$-wide YSi_2 nanowire. (C) Simulated filled-state STM image on a $3a_{Si}$-wide YSi_2 nanowire adopting the structure model as shown in Fig. 2(B). (D) Cross-sectional line profile on a $3a_{Si}$-wide YSi_2 nanowire.

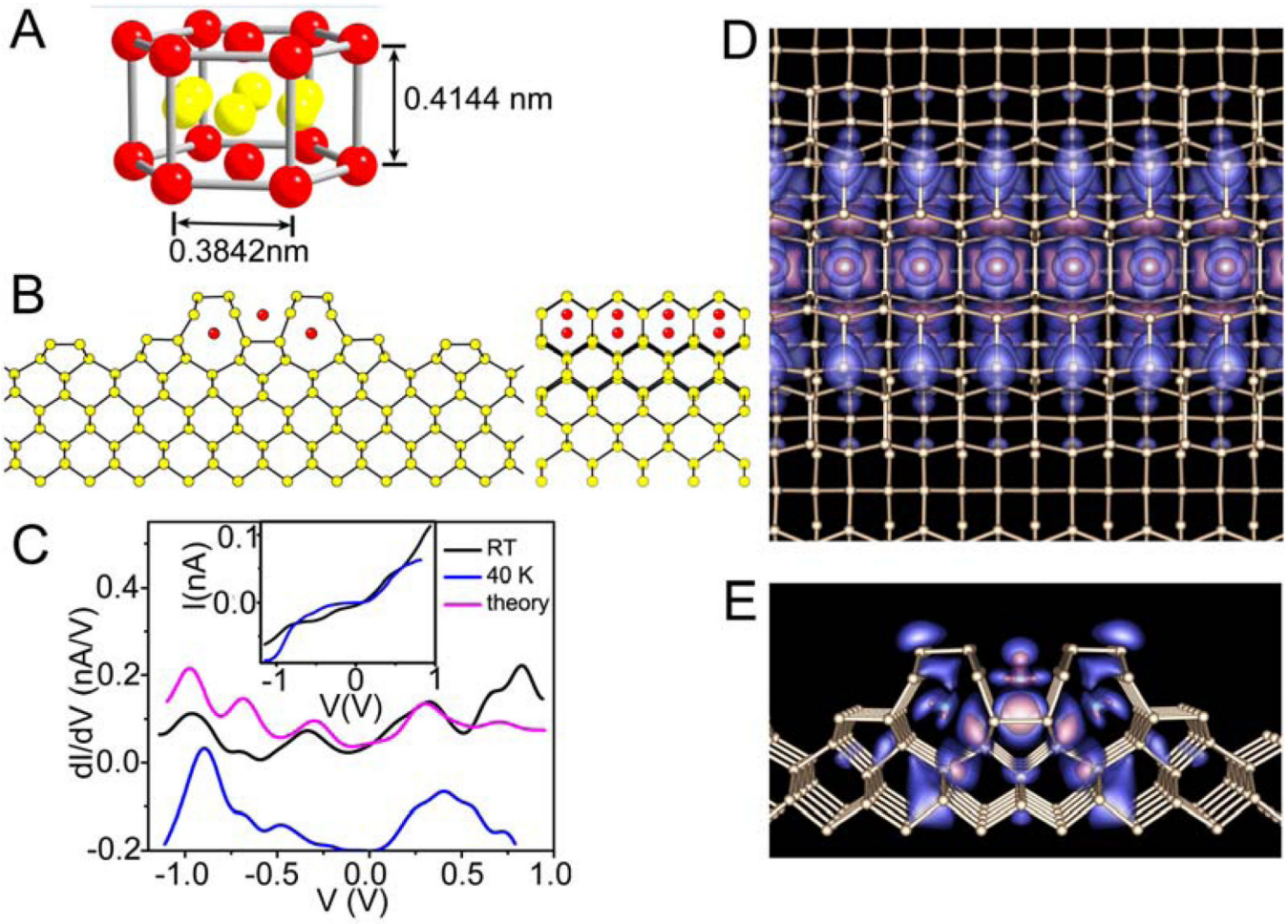

Fig. 2.

(A) Structure model of bulk YSi_2 with the hexagonal AlB_2 structure. The silicon atoms are shown in yellow while the yttrium atoms are in red. (B) Cross-sectional view and side view of the calculated structure of the thinnest, $3a_{Si}$-wide YSi_2 nanowires. (C) dI/dV spectra, obtained by numerical differentiation of the I–V spectra of the $3a_{Si}$-wide YSi_2 nanowires, recorded at RT (black) and at 40 K (blue). For clarity, the dI/dV spectrum at 40 K is offset by −0.2 nA/V. The raw I–V data are shown in the inset. The calculated surface DOS is shown in pink. (D and E) Top view and cross-sectional view of the calculated wave function densities on the $3a_{Si}$-wide YSi_2 nanowire. Blue and magenta represent 30% and 70% wave function density isosurfaces.

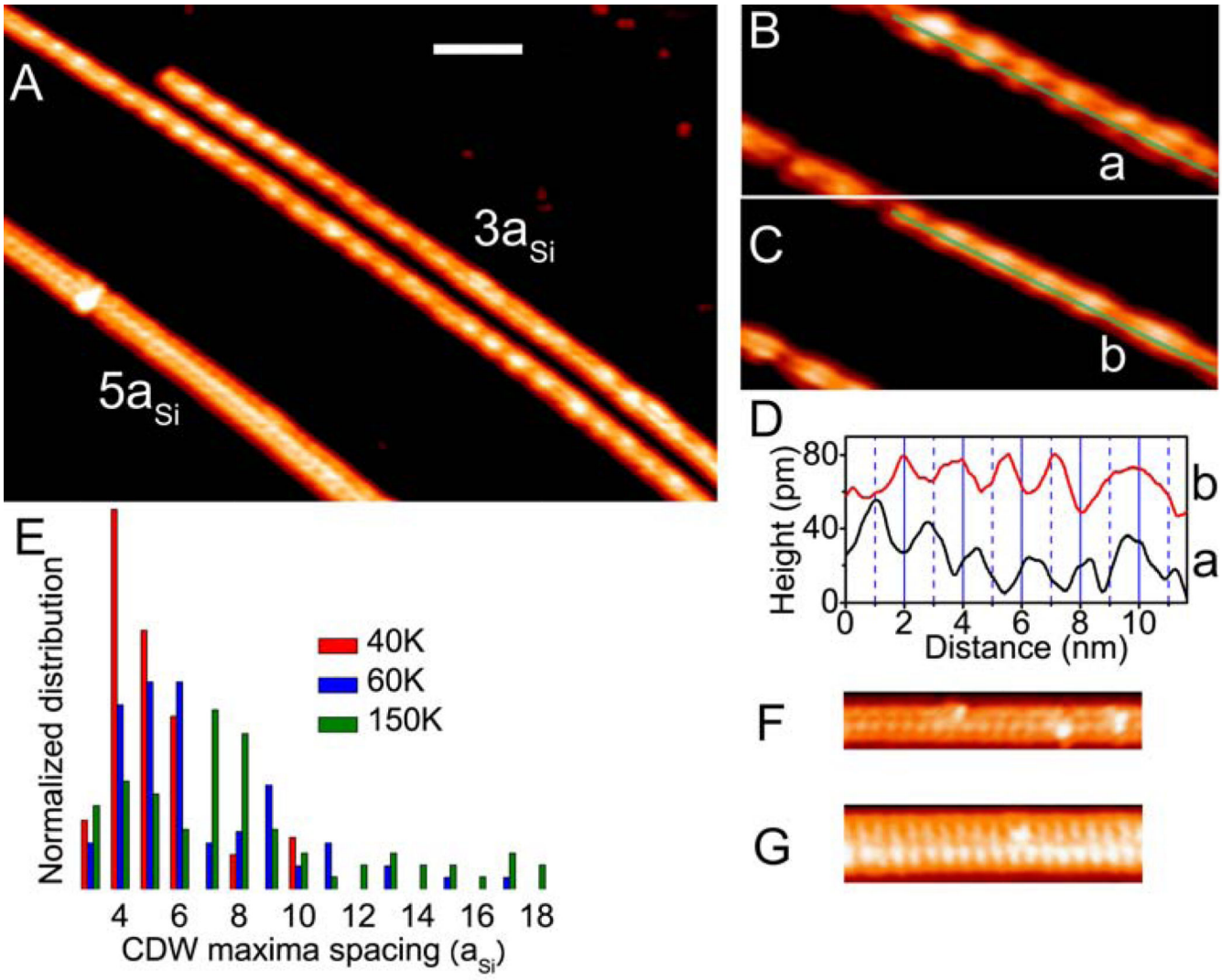

Fig. 3.

(A) STM image (V_s = −1.2 V) scanned at 40 K. The scale bar represents 5 nm. (B) and (C) are registry aligned dual bias STM images scanned simultaneously at 40 K with a sample bias of −0.8 V and 0.8 V, respectively. The bright protrusions indicate a charge ordering pattern. (D) Line profiles along lines ‘a’ and ‘b’ in (B) and (C), respectively. The curves are shifted vertically for clarity. (E) Statistical distributions of the spacings between neighboring charge density maxima in filled-state STM images for different temperatures. (F and G) STM images of $5a_{Si}$-wide and $7a_{Si}$-wide YSi_2 nanowires at 40 K. The image widths in (F) and (G) are both 14 nm. There is no charge ordering.

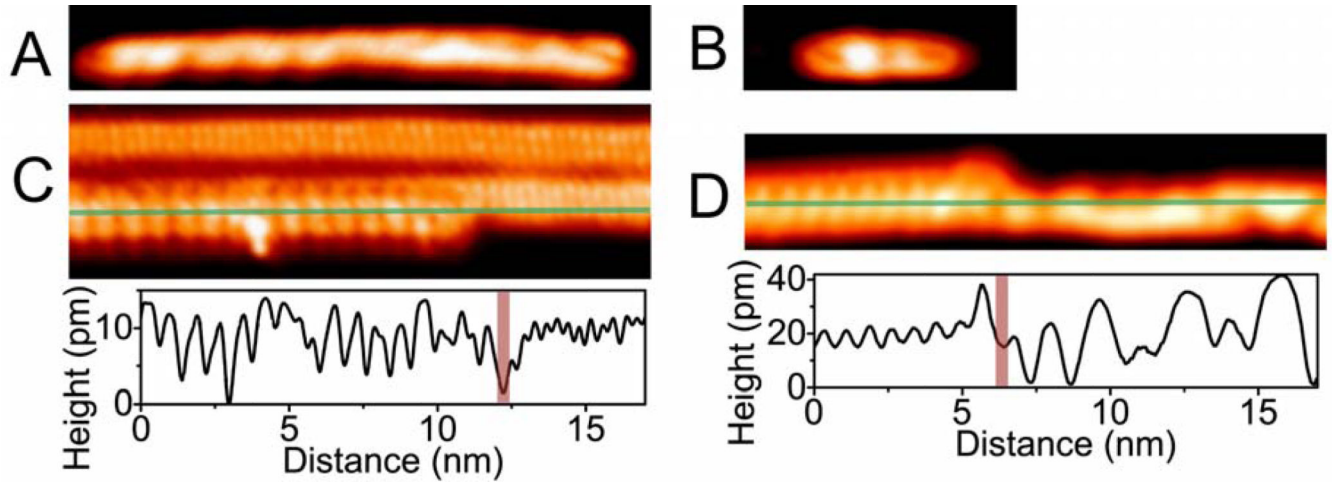

Fig. 4.

(A) and (B) Filled-state STM images of 16.9 nm and 4.6 nm long wire segments, scanned at 40 K. The bright protrusions form a charge ordering pattern. (C) Filled-state STM image showing an YSi_2 nanowire with a $3a_{Si}$–$5a_{Si}$ junction, scanned at RT. The bottom panel shows the STM line profile along the green horizontal line, revealing a period doubling on the $5a_{Si}$ wide side of the junction (not related to charge ordering). The approximate location of the junction is indicated by the vertical bar. (D) Filled-state STM image at 40 K, showing a $3a_{Si}$–$5a_{Si}$ junction. The bottom panel shows the corresponding line profile. The line profile reveals charge order fluctuations on the narrow (right) side of the junction.